Analysis of the Role of Digital Inclusive Finance in Promoting Regional Industrial Development Based on Multidimensional Data

Rui Ding, Qingjun Zeng
Chengdu Chongqing Economic Circle Construction Research Institute, Chongqing Technology and Business University, Chongqing 400067, China
Corresponding author: Rui Ding (e-mail: 18680753383@163.com)

ABSTRACT Understanding multidimensional interaction mechanisms and information propagation across interconnected regional networks has become increasingly important for coordinated industrial development and intelligent decision-making. To overcome the limitations of conventional spatial models based solely on geographic proximity, this study proposes a three-dimensional coupled analytical framework integrating geography, industrial linkages, and financial flows for investigating the impact of digital inclusive finance on regional industrial development. Geographic information, interregional input–output relationships, and intercity digital payment flows are fused through an entropy-weighted coupling strategy to construct a multidimensional spatial interaction matrix. Dynamic Spatial Durbin Models, spatiotemporal geographically weighted regression, and social network analysis are subsequently employed to characterize spillover mechanisms, transmission pathways, and core–periphery structures. Experimental results demonstrate that the proposed three-dimensional framework significantly enhances spatial spillover estimation, increasing the spillover coefficient from 0.263 to 0.384 while improving model explanatory power to an R^2 of 0.784. Financing constraint mitigation contributes 45% of the mediation effect, followed by technological innovation spillover and industrial linkage transmission. By modeling heterogeneous interaction networks and dynamic propagation behaviors, the proposed framework provides an effective computational paradigm for multidimensional information fusion and offers valuable engineering references for network topology optimization, distributed communication architectures, electromagnetic wave propagation modeling, and adaptive routing strategies in large-scale interconnected systems.

INDEX TERMS digital inclusive finance, multidimensional spatial networks, spatiotemporal information propagation, network topology analysis, electromagnetic wave propagation

I. INTRODUCTION

WITH its low cost, extensive scope, and efficient reach, digital inclusive financial services are a major factor in reshaping the development patterns of regions and their industries. Nevertheless, previous research examining the spatial spillover effects of digital inclusive finance tends to use only one type of geographical proximity (neighborhood) weight, or alternatively, use a simplistic economic distance measurement as the basis for analysis, and does not provide an adequate representation of the intricacies of the spatial linkage structure made up by the divisions of labour in the industrial chains or the capital flow networks [1,2]. Such a simplification can easily overlook the dynamic and directional characteristics of spatial flows, which leads to an inaccurate estimate of spatial spillover effects leading to an inaccurate identification of mechanisms of collaborative development at a regional industrial level [3,4].

In reality, regional industrial growth is based on many factors apart from just geography; it is also based on previous industrial activity (i.e., upstream and downstream) through the interactions of those industries' inputs and outputs. Regional growth is further affected by their financial network based on the flow of capital through those industries. Scholars both domestically and internationally have explored this from different dimensions. One study, based on panel data from prefecture-level cities, used a spatial Durbin model to verify the significant radiation effect of digital inclusive finance on the upgrading of manufacturing in surrounding areas; however, its weight matrix only relies on the inverse of geographical distance, failing to reflect the vertical linkages of the industrial chain [5,6]. Huang Y established a dual fixed effects model and a mediating effect model to examine the impact of digital inclusive finance on industrial integration and its path, and further explored the moderating role and spatial differences of financial support [7]. Chen Y studied the impact of digital inclusive finance on inter-city innovation cooperation, revealing that digital inclusive finance can significantly enhance the breadth and intensity of innovation cooperation [8]. Sun Z attempted to examine the spatial interaction effect between digital inclusive finance and technological innovation, that is, the impact of geographical location on the mechanism of their coordinated development [9]. Chen L explored the impact of digital inclusive finance and industrial structure upgrading on the economy, showing that the positive impact only appeared after financial and industrial development exceeded a certain threshold, and the spillover effect is more significant in non-central cities than in central cities [10]. The above studies have laid an important foundation for understanding the spatial effect of digital inclusive finance, but in the construction of the weight matrix, there are generally problems such as single dimension, subjective weighting, and failure to dynamically integrate the multiple interactions of "geography-industry-finance", which leads to limited estimation accuracy of spatial spillover effect and difficulty in capturing the real transmission process of spillover path in complex network.

To address the core deficiency of the single dimension of the weight matrix, some studies have attempted to directly improve the spatial weight setting. Janatabadi F introduced an accessibility weight matrix to capture the spatial dependence of accessibility within a region [11]. Other studies, while not directly improving the weight matrix, have revealed the multidimensionality and complexity of spatial dependence from the perspectives of spatial econometric analysis, regional difference decomposition, and threshold effect: Hui P analyzed how digital finance affects regional innovation capabilities through spatial econometrics and found that digital finance has a significant spatial spillover effect [12]; Dong H used centroid shift and Theil index decomposition to explore the regional differences in the development of inclusive digital finance [13]; Ding R and Chen L introduced environmental regulation variables into the spatial Durbin model and found that the spillover effect of digital finance has significant nonlinearity and spatial heterogeneity [14,15]. However, none of the above studies have achieved the organic integration of the three heterogeneous spatial structures of geographical proximity, industrial chain linkage, and financial flow dynamics, and lack in-depth analysis of the dynamic identification and non-stationarity characteristics of spatial spillover paths, making it difficult to reveal the differentiated transmission mechanism of inclusive digital finance in different spatial structures. Therefore, this paper aims to construct a three-dimensional coupled spatial analysis framework of "geographyindustry-finance" to address the estimation bias of spatial spillover effects caused by the coarse spatial weight matrix and neglect of the dynamics of financial flows in existing studies. The study first integrates geographic information of prefecture-level cities, inter-regional input-output tables, and intercity digital payment flow data to construct geographic proximity weight matrices, industrial chain association weight matrices, and financial flow weight matrices, respectively, and couples them into a comprehensive weight matrix using the entropy method. Then, a dynamic spatial Durbin model and spatiotemporal geographic weighted regression are employed, combined with social network analysis, to identify core-periphery structures and spillover paths. Based on this, the paper focuses on examining three transmission mechanisms by which digital inclusive finance promotes regional industrial development: relief of financing constraints, technological innovation spillover, and industrial association transmission. Through these methods, this paper reveals the transmission mechanism by which digital inclusive finance reshapes the regional industrial spatial pattern through financial flow networks, providing a theoretical basis for differentiated regional collaborative development policies.

II. METHOD

A. DATA PREPROCESSING AND CONSTRUCTION OF MULTIDIMENSIONAL INDICATOR SYSTEM

The study uses prefecture-level cities within China that had available data from 2015 through 2022. Any cities with missing data or that underwent significant changes in their administrative divisions are omitted from this dataset, resulting in 110 prefecture-level cities forming a balanced panel for evaluation. The balanced dataset includes observations from cities located in the eastern, central, western and northeastern regions of the country to provide a representative sample of spatial variation while maintaining continuity and comparability of the variable measurements over time. The data on which the research is based are derived from four primary sources: the Peking University Digital Inclusive Finance Index, the China Urban Statistical Yearbook, Interregional Input-Output Tables, and anonymized transaction data from leading thirdparty payment providers, including Alipay and WeChat Pay, which collectively account for over 90% of China's mobile payment market share. The dataset covers over 1.2 billion transaction records annually, ensuring high consistency with the Peking University Index in terms of digital service penetration and capital flow intensity, thereby providing a robust empirical foundation for the "geography-industry-finance" coupling and anonymized transaction records provided by the Digital Finance Research Center, covering the two dominant mobile payment platforms in China (Alipay and WeChat Pay) from 2015 to 2022. The dataset includes over 500 million annual inter-city capital transfer records. To construct the city-level financial flow matrix, we aggregated individual transaction-level data by summing the total volume of cross-city transfers between 110 sample cities. Data cleaning involved removing system-generated internal transfers and error logs to ensure the data reflected genuine economic activities. All personal identifiers were processed using a one-way cryptographic hash (SHA-256) at the source before being provided for research, strictly adhering to China's Data Security Law[16,17]. In order to manage the differences in dimensionality as well as the existence of nonstationarity in multiple dimensions , this study employs a logarithmic transformation for the positive skewness of some variables (such as digital payment transaction volume and patent authorizations): $y_{it}= \ln(x_{it}+\epsilon)$, where x_{it} represents the original observation value of the *i*-th city in year *t*, $\epsilon$is a smoothing constant, and y_{it} is the transformed sequence. This approach aims to reduce heteroscedasticity interference and improve model convergence stability.

Missing values are handled using a strategy combining multiple imputation and spatially weighted interpolation. For indicators with a random missing rate of less than 5%, five sets of complete data are generated using Multivariate Imputation by Chained Equations (MICE), and parameter estimates are merged using the Rubin rule [18]. For variables with spatial autocorrelation characteristics (such as the intensity of intercity capital flow), an inverse distance weight matrix is constructed, and the gaps are filled with the weighted mean of observations from neighboring cities to ensure that the spatial dependence structure is not destroyed. Indicator standardization adopted the range method to eliminate the influence of dimensions. Positive and negative indicators are processed according to the two equations of equation (1):

$$
\begin{aligned}
x'_{itj} &= \frac{x_{itj} - \min_j(x_j)}{\max_j(x_j) - \min_j(x_j)}, \\
x'_{itj} &= \frac{\max_j(x_j) - x_{itj}}{\max_j(x_j) - \min_j(x_j)}.
\end{aligned} \tag{1}
$$

In equation (1), x_{itj} is the original value of the j-th indicator in the t-th year of the i-th city, $\max_j(\cdot)$ and $\min_j(\cdot)$ are the global extreme values of the indicator within the sample period, and x'_{itj} is the standardized value mapped to the interval [0,1].

The multi-dimensional indicator system is constructed according to a three-level architecture of "target layer

- criterion layer - indicator layer". The digital inclusive finance dimension selects three criteria layers and 12 basic indicators: coverage breadth (account penetration rate, service outlet density), usage depth (average payment frequency, micro-credit availability), and digitalization level (mobile terminal usage rate, credit assessment coverage rate). The regional industrial development dimension covers three criteria layers and

11 basic indicators: industrial scale (total added value, employment absorption capacity), industrial structure (Theil index, advanced ratio), and industrial efficiency (total factor productivity, output per unit of energy consumption). Indicator weights are objectively assigned using the entropy method. The information entropy E_j and weight w_j of the j-th indicator are calculated as follows:

$$
\begin{aligned}
E_j &= -\frac{1}{\ln(TN)} \sum_{t=1}^{T} \sum_{i=1}^{N} p_{itj} \ln p_{itj}, \\
p_{itj} &= \frac{x'_{itj} + \delta}{\sum_{t=1}^{T} \sum_{i=1}^{N} (x'_{itj} + \delta)}, \\
w_j &= \frac{1 - E_j}{\sum_{k=1}^{M} (1 - E_k)}.
\end{aligned} \tag{2}
$$

In equation (2), T represents the time span, N represents the city sample size, M represents the total number of indicators, δ represents the zero-value correction term, p_{itj} represents the standardized weight, and w_j represents the final weight. This method avoids subjective weighting bias by measuring information dispersion, ensuring that the contribution of indicators is consistent with the data variation characteristics. The comprehensive index is synthesized using linear weighted aggregation: $I_{it} = \sum_{j=1}^{M} w_j x'_{itj}$, which yields the prefecture-level city digital inclusive finance index and industrial development index, respectively. To verify the internal consistency of the indicator system, Cronbach's α coefficient and variance inflation factor are calculated to eliminate multicollinearity interference.

B. SPATIAL WEIGHT MATRIX CONSTRUCTION

The geographic proximity weight matrix uses the spherical distance equation to calculate the great circle distance between the centroids of cities, thus eliminating planar projection errors. Let the latitude and longitude coordinates of cities i and j be (ϕ_i, λ_i) and (ϕ_j, λ_j) respectively, and the geographic distance d_{ij} is calculated according to the Haversine equation [19,20]:

$$
d_{ij} = 2R \cdot \arcsin\left(\sqrt{\begin{aligned}&\sin^2\left(\frac{\phi_j - \phi_i}{2}\right) \\ &+ \cos\phi_i \cos\phi_j \sin^2\left(\frac{\lambda_j - \lambda_i}{2}\right)\end{aligned}}\right). \tag{3}
$$

In equation (3), R is the average radius of the Earth, and the angles are uniformly converted to radians. ϕ_i and ϕ_j represent the latitudes of city i and city j, and λ_i and λ_j represent the longitudes of city i and city j. The weight elements are set to exponential decay form, and the diagonal elements are forced to zero for standardization.

The industrial chain association weight matrix is constructed based on a multi-regional input-output table. First, the provincial department data is weighted and split to prefecture-level cities according to employment scale, and the inter-regional transaction flow is balanced using a dual-scale method [21,22]. The forward association strength F_{ij} and backward association strength B_{ij} of city i and j are calculated as follows:

$$F_{ij} = \sum_{s=1}^{S}\sum_{r=1}^{S} x_{is} \cdot a_{sr} \cdot z_{rj}, \quad B_{ij} = \sum_{s=1}^{S}\sum_{r=1}^{S} z_{is} \cdot a_{sr} \cdot x_{jr}. \tag{4}$$

In equation (4), x_{is} represents the total output of sector s in city i, z_{rj} represents the final demand of sector r in city j, a_{sr} represents the direct consumption coefficient matrix element, and S represents the total number of industrial sectors. The bidirectional correlation strength is calculated by taking the arithmetic mean and standardizing: $w_{ij}^{\mathrm{ind}} = (F_{ij} + B_{ij})/\max_{i,j}(F_{ij} + B_{ij})$, eliminating the difference in dimensions.

The financial flow weight matrix is constructed based on desensitized intercity digital payment transaction records. After spatiotemporal alignment, the original transaction logs are aggregated into the annual capital flow amount F_{ij} of the city. Capital flow is directional, so F_{ij} represents the annual capital flow amount from city i to city j, and F_{ji} represents the annual capital flow amount from city j to city i. To eliminate the city scale effect, a gravity model is used for standardization [23,24]:

$$w_{ij}^{\mathrm{fin}} = \frac{(F_{ij} + F_{ji})/\sqrt{V_i \cdot V_j}}{\sum_{l \neq i}(F_{il} + F_{li})/\sqrt{V_i \cdot V_l}}. \tag{5}$$

In equation (5), V_i represents the total financial flow of city i. l is the summation index, and F_{il} represents the total amount of digital payment funds flowing from city i to city l. This processing makes the weights reflect the relative strength of financial connections rather than the absolute scale, and satisfies the constraint that the row sum is 1.

The coupling of the three-dimensional weight matrices employs an information-theoretic entropy approach to determine the optimal contribution of each spatial dimension. To resolve the conceptual challenge of weighting relational matrices, we first flatten each N × N weight matrix (excluding diagonal elements) into a vector of dimension 1 × N(N-1) , representing the global distribution of spatial interaction intensity for that specific dimension.

The theoretical justification for using entropy weighting lies in its ability to objectively measure the "infor mation certainty" or "structural contrast" within each spatial structure. Dimensions with higher dispersion (lower entropy) provide more distinctive spatial information for identifying spillover boundaries and are thus assigned higher weights.

The information entropy H_k for the k-th dimension is calculated based on the probability distribution of its relational elements:

$$H_k = -\frac{1}{\ln Q}\sum_{i=1}^{N}\sum_{j=1}^{N} q_{ij}^{(k)} \ln q_{ij}^{(k)}, \quad q_{ij}^{(k)} = \frac{\widetilde{w}_{ij}^{(k)}}{\sum_{i,j}\widetilde{w}_{ij}^{(k)}}. \tag{6}$$

In equation (6), $Q = N(N-1)$ represents the number of effective city pairs. N is the total number of prefecture-level city samples. $q_{ij}^{(k)}$ is the proportion of $\widetilde{w}_{ij}^{(k)}$ among all off-diagonal elements in the k-th class weight matrix. By treating the flattened spatial relationships as realizations of a spatial process, this approach avoids the bias of subjective weighting while capturing the intrinsic variance of inter-city linkages. Since the entropy method of weighting depends on the data dispersion, although its results are objective, it may still show certain sensitivity to parameter settings and sample distribution in the context of multidimensional matrix coupling. Therefore, it is necessary to further examine the response characteristics of the comprehensive weight matrix to the weight perturbation of each dimension in order to evaluate the robustness of the model setting and the reliability of the interpretation. To this end, this paper constructs a continuous variation space of three-dimensional weight parameters to characterize the changing trends of key statistics of the comprehensive matrix (such as spatial autocorrelation coefficient and spectral radius) under different weight combinations, thereby forming a weight sensitivity surface. The sensitivity surface of the weight of the three-dimensional coupling matrix is shown in Figure 1.

Figure 1 shows the sensitivity surface of the weights in the three-dimensional coupling matrix. The spatial autocorrelation coefficient exhibits a decreasing trend from high to low. When the geographical weight increases and the industry association weight relatively decreases, the spatial autocorrelation coefficient weakens significantly, indicating that traditional geographical proximity still plays a dominant role in the spatial dependency structure. Meanwhile, the surface changes are relatively smooth without significant abrupt changes, indicating that the model's response to weight perturbations has continuity and stability.

C. SOCIAL NETWORK ANALYSIS

Based on the comprehensive weight matrix W^{comp}, a directed weighted network G= (V, E, Ω) is con structed, where the node set *V*corresponds to 110 prefecture-level cities, the edge set *E*consists of non-zero weight elements, and *Ω* is the weight mapping function. To eliminate the interference of network density on the centrality index, a threshold truncation method is used to retain the top 15% of strong connection edges to ensure the integrity of the topology [25,26].

The node centrality measure is comprehensively represented by the three-dimensional vector $C_i = (C_i^{\mathrm{out}}, C_i^{\mathrm{betw}}, C_i^{\mathrm{eig}})^\top$. The out-degree centrality C_i^{out} is directly taken as the row sum: $C_i^{\mathrm{out}} = \sum_{j \neq i} w_{ij}^{\mathrm{comp}}$, reflecting the city's capital radiation capacity. w_{ij}^{comp} is the final weight element between city i and city j in the three-dimensional coupled comprehensive weight matrix. The betweenness centrality C_i^{betw} is calculated by improving the Brandes algorithm, considering the path probability of edge weights [27]:

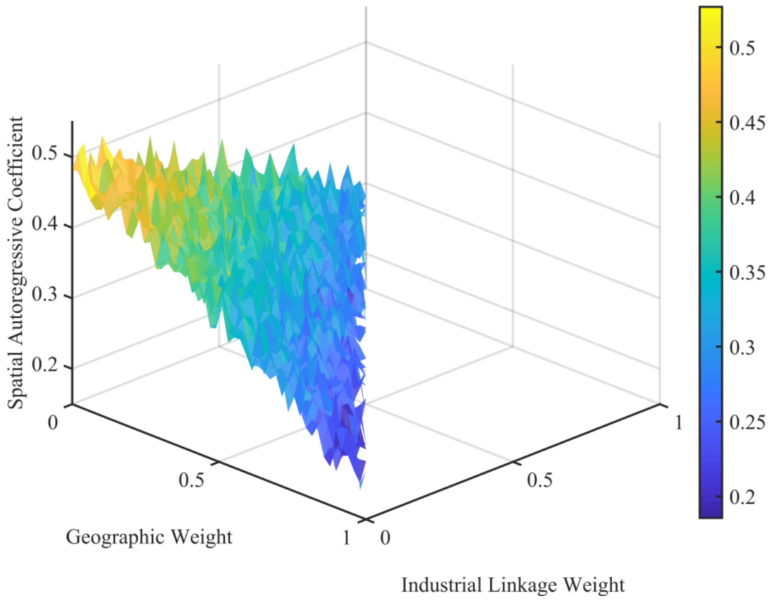

FIGURE 1. Sensitivity surface of the weights of the three-dimensional coupling matrix

$$C_i^{\text{betw}} = \sum_{s \neq i \neq t} \frac{\sigma_{st}(i)}{\sigma_{st}}, \qquad \sigma_{st}(i) = \sum_{p \in P_{st}} I(i \in p) \prod_{(u,v) \in p} w_{uv}^{\text{comp}}. \tag{7}$$

In equation (7), σ_{st} is the total number of weighted paths in the set P_{st} of all valid paths from node s to t, p is a specific path in the set, $\sigma_{st}(i)$ is the number of weighted paths passing through i, and $I(\cdot)$ is the indicator function. w_{uv}^{comp} is the weight of edge (u, v), and $\prod_{(u,v)\in p} w_{uv}^{\text{comp}}$ is the product of the weights of all edges on path p. This design makes the mediation effect not only dependent on the number of paths, but also reflects the cumulative contribution of the intensity of capital flow.

The eigenvector centrality C_i^{eig} solves for the principal eigenvector using the power iteration method. The iteration equation is:

$$c^{(n+1)} = \frac{W_{\text{comp}} c^{(n)}}{\|W_{\text{comp}} c^{(n)}\|_2}, \qquad C_i^{\text{eig}} = \lim_{n\to\infty} c_i^{(n)}. \tag{8}$$

$c^{(n)}$ is the feature vector centrality vector obtained in the n-th iteration, and the convergence criterion is $\|c^{(k+1)} - c^{(k)}\|_1 < 10^{-8}$. This index captures the association strength between nodes and their high-centrality neighbors, effectively identifying hidden hub cities.

Community partitioning uses the Louvain algorithm for modular optimization. The modularity Q is defined as the structural deviation between the actual network and the randomized configuration model [28,29]:

$$Q = \frac{1}{2\Omega_{\text{tot}}} \sum_{i,j} \left[w_{ij}^{\text{comp}} - \frac{\text{outdeg}_i \text{indeg}_j}{\Omega_{\text{tot}}} \right] \delta(\text{tag}_i, \text{tag}_j). \tag{9}$$

In equation (9), $\Omega_{\text{tot}} = \sum_{i,j} w_{ij}^{\text{comp}}$ represents the total network weight, $\text{outdeg}_i = \sum_j w_{ij}^{\text{comp}}$ and $\text{indeg}_j = \sum_i w_{ji}^{\text{comp}}$ represent the out-degree and in-degree strengths of the nodes, respectively, $\delta(\cdot)$ is the Kronecker function, and tag_i is the community label of node i. The algorithm performs a two-stage iteration: the first stage traverses the nodes and moves them into the neighboring communities that maximize the change in Q; the second stage aggregates the communities to generate supernodes and repeats the optimization until Q converges. After completing the calculation of the node centrality indices (out-degree centrality, betweenness centrality, and eigenvector centrality), it is necessary to further characterize the heterogeneity of the network structure from the perspective of overall distribution characteristics. Single mean or local indicators are difficult to reveal the stratification and concentration of influence between cities. Therefore, this paper introduces the Cumulative Distribution Function (CDF) to provide a global description of the centrality indices, as shown in Figure 2.

Figure 2 shows that the distribution of the three centrality indicators all exhibits a clear right-skewed charac teristic, meaning that most cities are concentrated in the lower centrality range, while a few nodes have a higher centrality level. This indicates a significant imbalance in the network structure, with a few core cities dominating capital flows and spatial spillovers. Meanwhile, the distribution curve of betweenness centrality is relatively steeper, indicating its more crucial role in network connectivity.

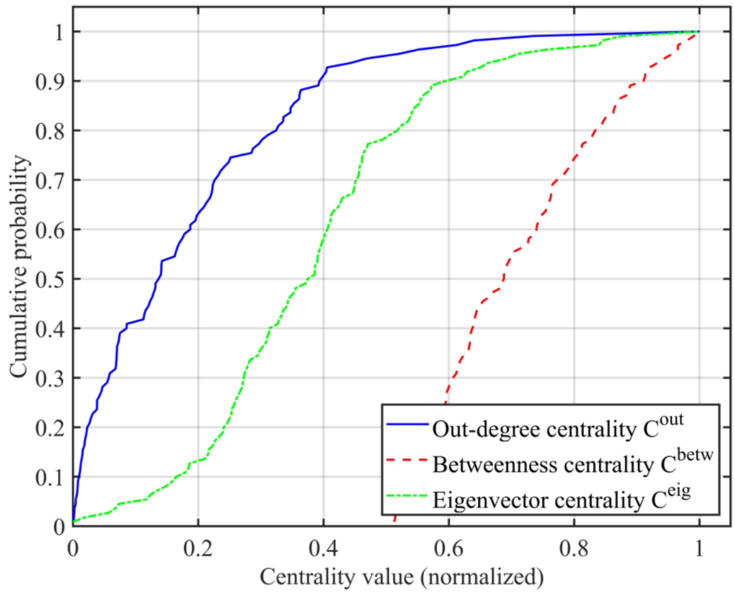

FIGURE 2. Cumulative distribution function of network centrality

Core-periphery structure identification employs a dual-threshold determination method. First, nodes are sorted in descending order by C_i^{eig}, and the top 20% quantiles are selected as the core candidate set. Second, the spillover contribution rate $\eta_i = C_i^{\text{out}} / \sum_{j\in C} C_j^{\text{out}}$ (where C is the candidate set) is calculated for each candidate node, and nodes with $\eta_i > 0.03$ are retained as core regions. Periphery regions are defined as nodes in the bottom 30% of the C_i^{betw} list that have no outgoing edges pointing to the core region; the rest are classified as semi-periphery regions. This strategy considers both the node's own influence and its network position, avoiding misjudgment based on a single indicator.

Spillover path identification is based on an improved K-shortest path algorithm. Using the core area as the source set and the edge area as the sink set, the weighted shortest path is calculated as $L_{st} = \arg\min_{p\in P_{st}} \sum_{(u,v)\in p} (w_{uv}^{\text{comp}})^{-1}$, and the flow betweenness of the high-frequency edge (u, v) is counted as $B_{uv} = \sum_{s,t} I((u, v) \in p) \cdot F_{st}$, where F_{st} is the amount of funds flowing from s to t.

D. DYNAMIC SPATIAL DURBIN MODEL SPECIFICATION

Based on the three-dimensional coupled spatial weight matrix W^{comp}, a dynamic spatial Durbin model is constructed to capture the spatiotemporal dependence and path dependence characteristics of regional industrial development, solving the problem that traditional static models neglect the inertia of industrial evolution and spatial feedback mechanisms [30,31]. The model specifications are as follows:

$$\begin{aligned} Y_{it} &= \tau Y_{i,t-1} + \rho \sum_{j=1}^{N} w_{ij} Y_{jt} + \beta X_{it} \\ &\quad + \theta \sum_{j=1}^{N} w_{ij} X_{jt} + \mu_i + \lambda_t + \epsilon_{it}. \end{aligned} \tag{10}$$

In equation (10), Y_{it} is the industrial development index of the i-th city in year t, $Y_{i,t-1}$ is the time lag term, τ is the time autoregressive coefficient, reflecting the path dependence strength of industrial development; w_{ij} is the element of the comprehensive weight matrix, $\rho$is the spatial autoregressive coefficient, measuring the spatial spillover effect; X_{it} is the vector of core explanatory variables and control variables, $\beta$is the corre sponding regression coefficient, $\theta$is the spatial lag term coefficient, capturing the spatial interaction influence of explanatory variables; $\mu_i$and $\lambda_t$represent individual fixed effects and time fixed effects, respectively, and $\epsilon_{it}$is the random disturbance term.

Parameter estimation adopts the maximum likelihood estimation method (MLE). Since the model includes time lag terms of the explained variables, traditional fixed effects estimators suffer from Nickell bias, leading to inconsistencies between $\tau$and ρestimates, and consequently, endogeneity bias. This study uses bias-corrected maximum likelihood estimators, eliminates individual effect interference through the lumped likelihood function, and uses eigenvalue decomposition to process the spatial Jacobian determinant. The loglikelihood function is constructed as follows:

$$\ln L(\delta) = -\frac{NT}{2}\ln(2\pi\sigma^2) + T\ln|I_N - \rho W_{\text{comp}}| - \frac{1}{2\sigma^2}\sum_{t=1}^{T}\zeta_t^\top\zeta_t. \tag{11}$$

In equation (11), δ is the set of parameters to be estimated, and $|I_N - \rho W_{\text{comp}}|$ is the spatial Jacobian determinant, used to correct the probability density distortion caused by spatial dependence. ζ_t is the error vector in year t. The optimization process adopts the BFGS (Broyden, Fletcher, Goldfarb, Shanno) quasi-Newton algorithm, with the gradient convergence threshold set to 10^{-6} and the iteration upper limit set to 1000 times to ensure the global optimal solution. Before estimation, the weight matrix is row-normalized to make its spectral radius equal to 1. Based on this, as long as the absolute value of the spatial autoregressive coefficient is less than 1, the spatial process can be guaranteed to meet the stationarity condition. Since the regression coefficients of the spatial econometric model cannot directly reflect the marginal effect, the partial differential method is used to decompose the effect. The model is written in matrix form $Y = (I_{NT} - \tau L - \rho W_{\text{comp}})^{-1}(\beta X + \theta W_{\text{comp}} X + \eta Z)$, and the direct and indirect effects of the r-th explanatory variable are calculated by the mean of the diagonal elements and the mean of the off-diagonal elements, respectively:

$$\text{Direct}_r = \frac{1}{N}\,\text{tr}(S_r(W_{\text{comp}}))\,, \quad \text{Indirect}_r = \frac{1}{N}\boldsymbol{\iota}_N^\top\left(S_r(W_{\text{comp}}) - \text{diag}(S_r(W_{\text{comp}}))\right)\boldsymbol{\iota}_N. \tag{12}$$

In equation (12), $S_r(W_{\text{comp}}) = (I_{NT} - \tau L - \rho W_{\text{comp}})^{-1}(I_{NT}\beta + W_{\text{comp}}\theta)$, where $\boldsymbol{\iota}_N$ is an $N \times 1$ unit vector. This decomposition quantifies the impact of local digital inclusive finance on local industries (direct effect) and its spillover to external industries through spatial networks (indirect effect).

To verify the rationality of the model specification, Wald test and LR (Likelihood Ratio) test are performed.

The null hypotheses are $H_0 : \theta = 0$ and $H_0 : \theta + \rho\beta = 0$, respectively. The test results rejected the null hypotheses ($p < 0.01$), confirming the necessity of the SDM (Spatial Durbin Model) model specification. Simultaneously, it is tested whether the spatial autoregressive coefficient ρfalls within the interval (-1, 1) to ensure the spatial process is stationary. Finally, the model passed the Hessian matrix positive definiteness test, with all eigenvalues greater than zero, confirming the concavity of the likelihood function and the robustness of the estimation results.

E. SPATIOTEMPORAL GEOGRAPHIC WEIGHTED REGRESSION MODEL

To capture the spatiotemporal non-stationarity of the impact of digital inclusive finance, a spatiotemporal geographic weighted regression model is constructed. The model allows the regression coefficients to dynamically change with geographic coordinates (u_i, v_i) and time coordinates t_i, overcoming the limitation of the global model's assumption of constant parameters [32,33]. The local regression equation is set as $y_i = \upsilon_0(u_i, v_i, t_i) + \sum_{m=1}^{p}\upsilon_m(u_i, v_i, t_i)x_{im} + \epsilon_i$, where y_i is the explained variable, x_{im} is the m-th explanatory variable, $\upsilon_m(\cdot)$ is the spatiotemporally variable coefficient, and ϵ_i is the error term. The weight matrix is constructed using a Gaussian kernel function, and the spatiotemporal distance metric combines Euclidean distance and time difference. To prevent bandwidth search bias caused by dimensional differences, the spatial and time coordinates are first standardized by range. The weight w_{ij} of the i-th sample to the j-th sample is calculated as follows:

$$w_{ij} = \exp\left[-\left(\frac{d_{ij}^S}{h_s}\right)^2 - \left(\frac{d_{ij}^T}{h_t}\right)^2\right]. \tag{13}$$

In equation (13), $d_{ij}^S = \sqrt{(u_i - u_j)^2 + (v_i - v_j)^2}$ is the standardized spatial distance, $d_{ij}^T = |t_i - t_j|$ is the standardized time interval, and h_s and h_t are the spatial and temporal bandwidth parameters, respectively. Bandwidth determines the decay rate of the kernel function, directly affecting the local sample participation. If h_s is too small, the local variance is too large; if it is too large, it degenerates into a global model. In this paper, the method for optimizing bandwidth employs minimizing the adjusted Akaike information criterion. A grid search mode is employed to search through the combination of h_s and h_t in increments of 0.1. The objective function has been defined as follows:

$$\text{AICc} = 2g\ln(\hat{\sigma}) + g\ln\left(\frac{g + \text{tr}(D)}{g - 2 - \text{tr}(S)}\right). \tag{14}$$

In equation (14), g represents the total sample size, $\hat{\sigma}$ is the estimated standard deviation of the error, and $\text{tr}(D)$ is the trace of the hat matrix D, representing the effective degrees of freedom of the model. This criterion balances goodness of fit with model complexity, avoiding overfitting.

Locally weighted least squares are used to estimate the parameters. At every spatial and temporal coordinate, a diagonal weight matrix $W(u_i, v_i, t_i)$ is created. After the parameter estimation is done, the prediction accuracy is assessed using leave-one-out cross-validation. The variance inflation factor of each local regression equation is calculated to remove any interference caused by multicollinearity and to eliminate any outliers from the data.

III. EXPERIMENTS AND VERIFICATION

A. EXPERIMENTAL DESIGN

Data from 110 prefecture-level cities across China's four major geographical regions are selected for the period 2015–2022. The selection logic follows a dual-filtering approach: first, prioritizing cities with complete longitudinal data across the "geography-industry-finance" dimensions to ensure balanced panel integrity; second, maintaining a stratified representative distribution where the sample includes 40% of cities from the Eastern region, 30% from Central, 20% from Western, and 10% from Northeastern, closely reflecting the actual regional economic density of China. Cities excluded (approximately 180) primarily consist of those with fragmented digital transaction records or those that underwent administrative boundary adjustments, which would otherwise introduce measurement errors. This refined sample provides a balanced panel while mitigating potential selection bias. The primary driver of the analysis is the Peking University Digital Inclusive Finance Index, which collects data from microtransactions such as third-party payments and online loans, taking into account the three aspects of coverage, usage, and digitalization, and providing an accurate depiction of how developed digital finance is in each of the cities.

The dependent variable used in this study is a composite index of regional industrial development created using the entropy method, which synthesizes three different indicators of industrial development: scale of industry; structure of industry; and productivity of industry. There are four control variables used: the level of economic development in the region (measured as the log of GDP (Gross Domestic Product) per capita); the level of government involvement (measured as total fiscal expenditure divided by total GDP); the physical and optimal distribution of resources to support innovation (measured by the number of students enrolled in post-secondary institutions relative to the total population); and the availability of infrastructure to support effective transportation (measured as the total number of road miles developed for every 10,000 residents, plus the total number of broadband access points). The four control variables are statistically trimmed at the one percent level in order to eliminate any effects from extreme observations. Descriptive statistics on all of the key variables used in this study can be found in Table 1.

The results from 880 observations taken from 110 prefecture-level cities between 2015 and 2022 across all five dimensions are presented in Table 1. The data distribution demonstrates distinct hierarchical levels of differentiation across all five measurements. The main measure of digital inclusiveness—the Digital Inclusive Finance Index—is calculated at a mean of 186.42, with a standard deviation of 78.35. The range of values (43.21 to 412.67) shows significant variation between minimum and maximum values; therefore, the digital finance development levels vary substantially across all participating prefecture-level cities. Many prefecturelevel cities with low digital finance development levels are still at the beginning stages of developing their digital finance system, while some of the top performing cities are in an advanced stage of development. The measure of regional industrial development—the Regional Industrial Development Composite Index—has a mean of 0.412, with a standard deviation of 0.187. For the control variables, the log of per capita GDP averages 10.823 with a standard deviation of 0.631, indicating a relatively narrow distribution. Thus, while the levels of economic development among the sample cities vary from city to city, they fall within an approximate range of comparable levels of economic development. For example, the mean score on government intervention is 0.184, with a maximum of 0.423, suggesting a relatively high proportion of fiscal expenditures to GDP in some cities, which reflects the underdeveloped nature of the western region in which many of the sample cities are located and, therefore, a relatively high level of reliance on government transfer payments by these cities. The average of the indicators of human capital is 0.037, with a standard deviation of 0.021 and a minimum value of 0.004. There are very few higher education resources available in some cities compared to the others, and hence the differences in the distribution of innovation factors across geographical regions should not be overlooked. The Hadlock-Pierce Financing Constraint Index has an average value of -3.847, with a standard deviation of 0.412 which indicates there are significant differences in the financing constraints faced by different groups of enterprises located in different cities. The logarithm of the Technological Innovation Index has an average value of 2.143 but a minimum value of 0, this indicates that during the sample period some cities had extremely low patents granted. The Industrial Linkage Index has an average value of 0.523, ranging from 0.112 to 0.941. The minimum and maximum values indicate that there is a structural gap between the two cities with respect to the depth of the industrial chain nested within them.

B. SPATIAL AUTOCORRELATION TEST AND BENCHMARK REGRESSION

The baseline regression uses a dynamic spatial Durbin model configured with a three-dimensional coupling weight matrix to estimate how digital inclusive finance directly affects industrial development, and how it also creates spillover (indirect) effects on the regions surrounding the digital inclusion impact regions. The model comparison portion of the study systematically evaluates five different settings for the spatial weight matrix: the geographical proximity matrix, the geographical distance matrix, the industrial chain correlation matrix, the financial flow matrix, and the three-dimensional coupling matrix. For each of the five spatial weight matrix settings, one run of the dynamic spatial Durbin model is conducted to derive the spatial autoregression coefficient ρ, and to calculate the spatial spillover effects of each of the core variables. Furthermore, the sign, significance, and economic meaning of the spatial spillover coefficients in each of the five weight matrix settings are compared to identify how sensitive the estimation results are to the choice of weight matrix. Simultaneously, the goodness-of-fit R^2 of each model is calculated as a quan-t itative basis for model fitness. A pseudo- R^2 measure is u sed for goodness-of-fit. The log-likelihood value is directly o utput from the maximum likelihood estimation process; a

TABLE 1. Descriptive statistics of key variables

Variable Type	Variable Name	Observations	Mean	SD	Min	Max
Core explanatory variable	Digital Inclusive Finance Index	880	186.42	78.35	43.21	412.67
Dependent variable	Regional Industrial Development Composite Index	880	0.412	0.187	0.000	1.000
Control variable	GDP per capita (log)	880	10.823	0.631	9.214	12.347
Control variable	Government intervention degree (fiscal expenditure/GDP)	880	0.184	0.072	0.061	0.423
Control variable	Human capital (share of university students)	880	0.037	0.021	0.004	0.112
Control variable	Infrastructure composite index	880	0.318	0.156	0.000	1.000
Mediator variable	Financing constraint (Hadlock and Pierce Financial Constraint Index)	880	-3.847	0.412	-5.123	-2.314
Mediator variable	Technological innovation (patent grants per capita, log)	880	2.143	1.027	0.000	5.812
Mediator variable	Industrial linkage index	880	0.523	0.184	0.112	0.941

larger value indicates a stronger explanatory power of the model. To balance goodness-of-fit and model complexity, the AIC (Akaike Information Criterion) is further calculated, imposing a penalty term on coupling matrix models with more parameters to avoid overfitting. Figure 3 shows the spatial effect coefficient, the comparison of model goodness-of-fit, and the information criterion.

Figure 3 systematically evaluates the substantial impact of five types of spatial weight matrix settings on the identification results of spillover effects of digital inclusive finance by using spatial effect coefficients and model fit goodness. In Figure 3(a), both curves show a monotonically increasing trend from the geographic proximity matrix to the three-dimensional coupling matrix, but the increase in the spatial spillover coefficient is much more significant than that of the spatial autoregression coefficient ρ, revealing the high sensitivity of the weight matrix setting to spillover path identification. Specifically, the spillover coefficient under the geographical proximity matrix is only 0.263, and ρ is 0.134. After introducing the geographical distance matrix, the two coefficients slightly increase to 0.271 and 0.142, with limited improvement. However, after switching to the industrial chain correlation matrix, the spillover coefficient jumps to 0.325, and ρ rises to 0.176, indicating that the spatial dependence information contained in the vertical correlation of the industrial chain has surpassed the characterization ability of geographical distance. The financial flow matrix further pushes the spillover coefficient to 0.372, and ρ reaches 0.203, verifying the key role of intercity capital flow in spatial transmission paths. Under the three-dimensional coupling matrix, the two coefficients reach 0.384 and 0.218 respectively, which are the highest levels among all settings. The goodness-of-fit and AIC information criterion curves in Figure 3(b) exhibit a mirror cross structure: R^2 continuously climbs from 0.691 in the geographic proximity matrix to 0.784 in the three-dimensional coupling matrix, while AIC simultaneously decreases from 3740 to 3455. The inverse movement of the two curves is particularly steep in the interval between the financial flow matrix and the three-dimensional coupling matrix, indicating that the explanatory power gain brought by incorporating multidimensional spatial information is sufficient to cover the penalty term imposed by the increase in model complexity, and the statistical necessity of the multidimensional coupling design is fully supported. In terms of model autocorrelation test, Moran's I exponent of the residuals under each setting is calculated [34,35]. The construction of the Moran scatter plot is based on the standardized digital inclusive finance index, that is, the original index is centered so that the variable values are distributed around the zero value; at the same time, a spatial lag term is introduced to reflect the weighted average level of the surrounding areas of each city. The horizontal axis and the vertical axis correspond to these two variables respectively, and the slope of the scatter fitting line is the global Moran exponent, which is used to judge the direction and significance of spatial dependence. The Moran scatter plot is shown in Figure 4.

In Figure 4, Moran scatter plots for three years (2015, 2019 and 2022) demonstrate the dynamic changes in the spatial autocorrelation of digital inclusive finance index. The horizontal axis of the three sub-graphs is the z-value of the digital inclusive finance index, while the vertical axis is the value of the corresponding spatial lag term (Wz). The slope of the red fitted line is the global Moran index. According to Figure 4(a) in 2015, the Moran index is 0.1359, with a gentle slope of the fitted line and distance of the scatter points from the origin. There are no distinct clustering patterns among the scatter points in the 1st and 3rd quadrants (high-high clusters and low-low clusters), resulting in a weak positive spatial correlation signal at that time. Therefore, at that time the spatial distribution of digital inclusive finance is randomly (or nearly randomly) distributed throughout the geographies represented in this study, with little or no linkage effect between adjacent cities. Figure 4(b) shows that by 2019, the Moran Index had risen to 0.2680, with a significant increase in the slope of the fitted line. The clustering trend of scatter points along the diagonal direction of the first and third quadrants began to emerge, and the spatial dependence structure began to take shape. In Figure 4(c), the Moran Index further rose to 0.4376 in 2022, with the highest slope of the fitted line among the three sections. The spatial pattern of high-value clustering around high-value cities and low-value continuation around lowvalue cities became increasingly distinct. Meanwhile, the distribution range of the spatial lag term expanded from (-1.3410, 1.6902) in 2015 to (-1.4660, 1.9707) in 2022, while the distribution range

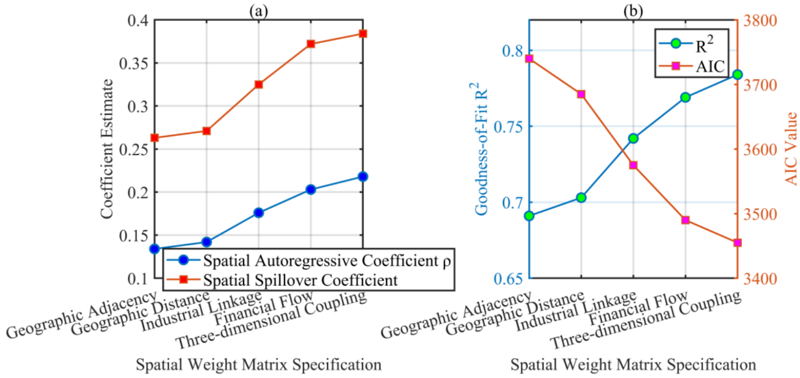

FIGURE 3. Comparison of benchmark regression and model results: (a) Comparison of spatial effect coefficients; (b) Comparison of model goodness of fit and information criterion

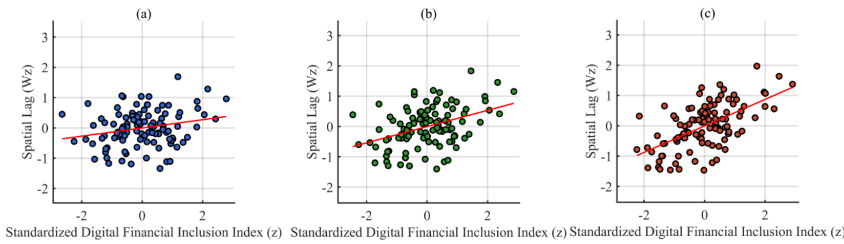

FIGURE 4. Moran Scatter Plot: (a) 2015; (b) 2019; (c) 2022

of the standardized digital inclusive finance index changed from (-2.6473, 2.7814) to (-2.2380, 2.9060). Both reveal that the individual differentiation in the development of digital finance within cities is intensifying, while the radiation capacity of core cities to their surrounding areas continues to strengthen, and the gap between peripheral cities and the core is further widening. The spatial dependence structure is gradually moving towards a coreperiphery characteristic.

Testing the Mediation Effect of the Spatial Spillover Transmission Mechanism

To identify the specific transmission paths through which digital inclusive finance impacts regional industrial development, this section constructs a spatial mediation effect model for mechanism testing. Based on the dynamic spatial Durbin model framework, maintaining consistency between the spatial weight matrix and control variable settings and the baseline regression, three mediating variables are introduced sequentially: financing constraint mitigation, technological innovation spillover, and industrial linkage transmission. The mediation effect is then decomposed into direct and indirect effects. In the spatial mediation effect model, the direct mediation effect reflects how local digital finance influences local industries through local mediating variables, while the indirect mediation effect captures how local digital finance influences mediating variables in neighboring regions through spatial spillovers, and then feeds back to the local area or influences industries in neighboring regions. The proportion of the mediation effect is used to quantify the contribution of different transmission mechanisms. The proportion of the mediation effect and the results of direct and indirect effects are shown in Figure 5.

Figure 5 systematically presents the three transmission paths and their internal mechanisms of digital inclusive finance's impact on regional industrial development from two dimensions: the proportion of mediating effects and the structure of direct-indirect effects. Figure 5(a) shows that the financing constraint mitigation path dominates with a proportion of 45%, the technology innovation spillover path contributes 30%, and the indus trial linkage transmission path accounts for 25%, with the three paths together forming a complete mediating effect system. However, simply ranking them by proportion would obscure the structural differences shown in Figure 5(b). The three paths exhibit different distribution patterns between direct and indirect mediating effects. The financing constraint path has the largest absolute magnitude of direct mediating effect at 0.2 (standard error 0.03) and indirect mediating effect at 0.25 (standard error 0.035). The technology innovation spillover path has a direct mediating effect of 0.08 (standard error 0.02) and indirect mediating effect of 0.22 (standard error 0.03), with the indirect effect far exceeding the direct effect, indicating a strong spatial dependence in the cross-regional diffusion of knowledge and technology. The direct mediating effect of the industrial linkage transmission path is 0.1 (standard error 0.025), and the indirect mediating effect is 0.15 (standard error 0.028). The standard error of the indirect effect is the smallest among the three, reflecting that this path has the highest estimation accuracy, but its absolute strength is relatively limited among the three. This result indicates that the spatial transmission effect of industrial

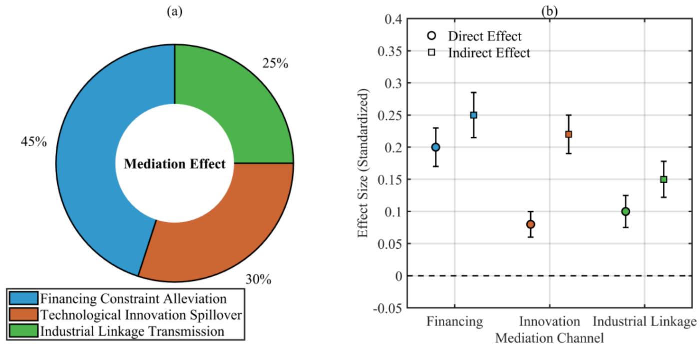

FIGURE 5. Decomposition results of mediation effect: (a) Proportion of mediation effect; (b) Comparison of direct and indirect mediation effects

chain linkages may depend on the existing network density, and the release of the effect in sparsely connected areas faces structural constraints.

C. HETEROGENEITY ANALYSIS OF CORE-PERIPHERY STRUCTURE

Out of the total of 110 prefecture level cities, they have been further classified into three distinct areas: core other semi-periphery and peripheral areas. In order to assess heterogeneity among these areas by conducting a grouped regression analysis using dynamic spatial Durbin models, a separate model is carried out for each of the three regions. The specifications for the models as well as the weight matrices, control variables, and method of estimation are all consistent with the benchmark regression so that coefficients could be compared across each region. After each regression, partial differential equations are used to decompose the effects, calculating the direct, indirect, and total effects of digital inclusive finance. The direct effect reflects the marginal impact of local digital finance development on local industrial upgrading; the indirect effect captures spillover feedback to external regions through spatial networks; and the total effect is the sum of the two. The distribution of effects among the core-periphery groups is shown in Figure 6.

Figure 6 systematically reveals the inherent differentiation logic of the heterogeneous impact of digital inclusive finance under the core-periphery structure from two dimensions: effect structure and geographicnetwork intersection. The most noteworthy aspect of Figure 6(a) is not the hierarchical difference in the total effect, but rather the deep divergence in the effect composition among the three types of regions: the average direct effect in the core region is 0.1375, in the semi-periphery region it is 0.1648, and in the periphery region it is 0.1462, all highly similar; however, the indirect effect shows a significant magnitude difference, with the average indirect effect in the core region reaching 0.3772, in the semi-periphery region 0.1710, and in the periphery region only 0.0661. This structure directly determines the gap in the total effect: the average total effect in the core region is 0.5147, while in the periphery region it is only 0.2123, with the spillover contribution systematically shrinking as network position decreases, and the direct effect becoming the main source of the effect in the periphery region. Figure 6(b) further amplifies this spatially nested characteristic of differentiation through a geographic-network cross-perspective: the total effect of the core cities in the east reaches 0.68, the central core is 0.45, and the western core is 0.39, showing a certain gap in the effects among the core cities of the three regions (0.68, 0.45, 0.39); while the differences among peripheral cities in the east, central, and western regions are limited (0.18, 0.22, 0.19). This means that the differences in geographical location are mainly reflected in the core layer rather than the peripheral layer. The 0.49 difference in total effect between the eastern core and the western periphery stems from the former's overwhelming spillover radiation capacity, rather than the simple advantage of local financial penetration.

D. SPATIOTEMPORAL EVOLUTION ANALYSIS

Before delving into the spatiotemporal evolution analysis, it first examines the overall evolution of the digital inclusive finance index from a macro-distribution perspective. Figure 7 presents the kernel density estimation results of the Peking University (PKU) digital inclusive finance index in 2015 and 2022.

As shown in Figure 7, the distribution curve shifted significantly to the right from a narrow peak with a mean of 170.23 (σ=19.25) to a mean of 285.95 (σ=24.90). While the overall development level improved, the absolute differences between regions slightly widened. However, the change in the peak value and the narrowing tail initially showed signs of convergence. This macro-distribution characteristic provides a descriptive statistical benchmark for further in-depth analysis of the temporal evolution and spatial diffusion paths of the coeffi cients.

Based on the estimation results of the spatiotemporal geographic weighted regression model, the regression coefficients of digital inclusive finance for 110 prefecture-level cities from 2015 to 2022 are extracted and summarized according to direct effects and spatial spillover effects. The annual mean is calculated using a simple arithmetic mean, the standard deviation reflected the dispersion of the coefficients, and the coefficient of variation (the ratio of

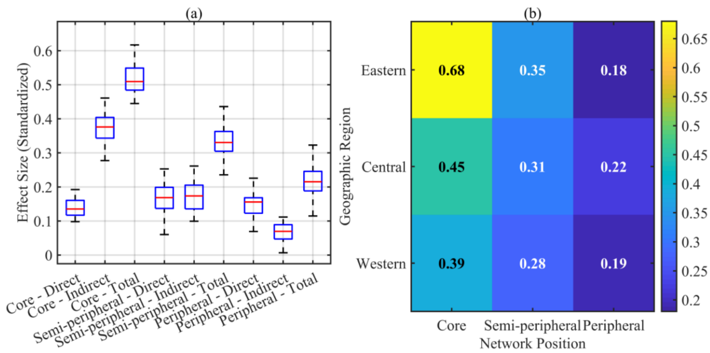

FIGURE 6. Heterogeneity analysis of the core-periphery structure: (a) Distribution of effects among core-periphery groups; (b) Effects by region and network location

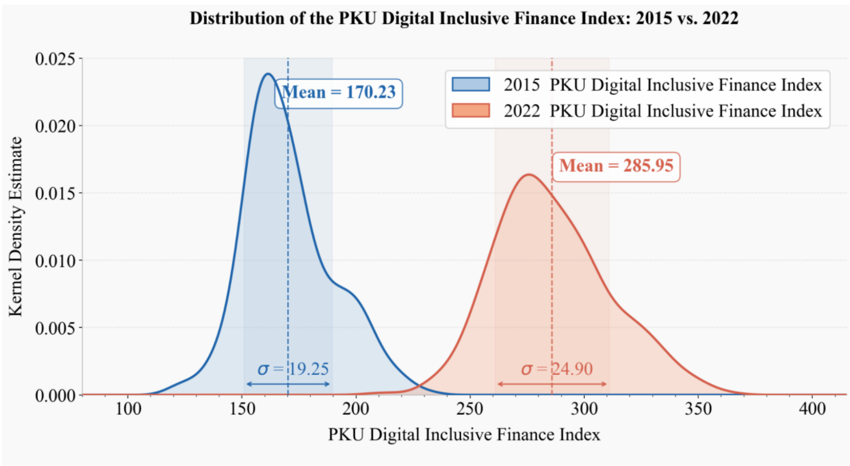

FIGURE 7. Kernel density estimation plot

the standard deviation to the mean) is used to compare the dynamic changes in regional differences after eliminating the influence of dimensions. All statistics are sampled 1000 times using the Bootstrap method to obtain confidence intervals, ensuring the robustness of the inference.

By comparing the annual mean changes of direct effects and spatial spillover effects, the temporal evolution trend is illustrated. The evolution of regional differences is measured using the Theil index. The Theil index is decomposed into within-group differences and between-group differences, with between-group differences calculated according to the eastern, central, and western geographical regions to identify the dynamic process of coordinated regional development. The weighted algorithm, which considers the ratio of city industrial added value to each year, so don't overlook the disparity of economic size between cities. Then using kernal density estimation to visualise how the spatial pattern developed. Each city's coefficient/year corresponding to geographic coordinates, producing a continuous density surface through a Gaussian Kernel function with adaptive bandwidth, enables analysis of the variability in isoline distribution over time. To ensure proper use of bandwidth selection employ Silverman's rule which creates an optimal balance of smoothing and mainte nance of detail. The spatiotemporal evolution of the spillover effects of digital inclusive finance is shown in Figure 8.

Figure 8 systematically depicts the spatiotemporal evolution of the spillover effects of digital inclusive finance from 2015 to 2022 from four dimensions. Figure 8(a) reveals the most theoretically significant structural shift: the mean of the direct effect increased from 0.214 to 0.397, while the mean of the spatial spillover effect increased from 0.153 to 0.408, forming a new pattern of "spillover dominance." Simultaneously, the standard deviations of both types of effects continued to narrow, with the standard deviation of the direct effect decreasing from 0.042 to 0.030 and the standard deviation of the spillover effect decreasing from 0.061 to 0.036, indicating that the intensity of the effects in different cities tends to concentrate, and the heterogeneity of responses between regions is being systematically compressed. From Figure 8(c), it can be concluded that the coefficient of variation decreased from 0.62 to 0.38, with a smooth trajectory of convergence. Figure 8(b) also shows the features of structural convergence through Theil Index Decomposition. The overall Theil Index decreases from 0.145 to 0.094, while the inter-group difference decreases from 0.060 to 0.027, and the intra-group difference decreases from 0.085 to 0.067. Therefore, the eastern, central, and western regions of the country are closing their respective development gaps quickly; however,

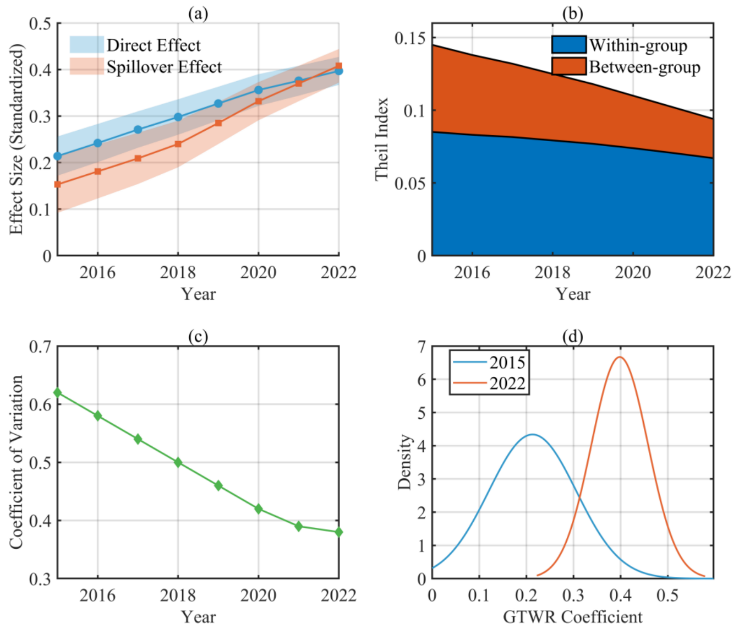

FIGURE 8. Spatiotemporal Evolution of Spillover Effects of Digital Inclusive Finance: (a) Temporal Evolution of Direct and Spillover Effects; (b) Evolution of Regional Differences: Theil Index Decomposition; (c) Convergence of Spillover Effects in Different Regions; (d) Kernel Density of Spillover Effects

the inter-cities differentiation within the same region is now the primary contradiction to regional balance. Micro-level evidence of this phenomenon can be found in the GTWR (Geographically and Temporally Weighted Regression) coefficient distribution depicted in Figure 8(d). For example, in 2015, the minimum coefficient is found to be 0; thus, the marginal impact of digital inclusion on industrial development in some cities is virtually non-existent. In 2022, the minimum coefficient increases to 0.222, indicating that all cities sampled have exceeded the required effect threshold; additionally, the maximum coefficient moderates from 0.597 to 0.579 and the standard deviation reduces from 0.093 to 0.060.

The spillover effect surpassing the direct effect in 2022 is not accidental; it reflects a deep structural shift in the mechanism of digital inclusive finance. In its early stages, the marginal benefits of financial coverage primarily impacted the local area. The direct easing of corporate financing constraints and the expansion of local payment scenarios drove immediate accumulation of industrial capital, allowing the direct effect to lead in the early stages. However, with the accumulation of platform network externalities, the scale and frequency of cross-city capital flows continued to rise.

E. ROBUSTNESS AND ENDOGENEITY TESTS

To verify the reliability of the baseline regression results, five tests are performed sequentially. The first test replaced the explained variable with total factor productivity (TFP) instead of the comprehensive industrial development index. TFP is calculated using the DEA (Data Envelopment Analysis)-Malmquist index method. Input indicators included capital stock and labor force, while output indicator is regional GDP. The global production frontier is calculated under a variable returns to scale setting. The regression model specification and control variables remained consistent with the baseline, and the signs, significance, and magnitudes of the coefficients of the core explanatory variables and spatial spillover effects are compared.

The second test replaced the spatial weight matrix and binarized the three-dimensional coupling matrix. Nonzero elements of the weights are retained and uniformly assigned a value of 1 to eliminate the potential influence of differences in weight strength on the estimation results. The dynamic spatial Durbin model is rerun to test whether the spatial spillover coefficients remained significant and consistent in direction. The third measure employs a two-stage least squares method to mitigate endogeneity bias. The interaction term of telephone penetration rate and previous year's internet user density in each city is selected as the instrumental variable for the digital inclusive finance index. The correlation assumption is satisfied by the historical communication infrastructure and is independent of current choices regarding industrial upgrading. The two-stage least squares method involves regressions in the first stage of the instrumental variable on the principal explanatory variable and in the second stage using fitted values for regression.

Using the System GMM method for estimating the dynamic panel model is the fourth way. For the purpose of estimating a non-spatial dynamic panel model with time lags, a simpler version of the dynamic spatial Durbin model is created by introducing a first-order lag term for each of the explanatory variables as an additional instrument to control for individual fixed effects and serial dependence on the noise.

The fifth measure excludes the samples from the four municipalities of Beijing, Shanghai, Tianjin, and Chongqing. The administrative level and resource allocation capacity of these municipalities are higher than those of ordinary prefecture-level cities, which may have a leverage effect on the estimation results. Regres sion is performed again based on the remaining 106 cities to compare the stability of the coefficients. The robustness and endogeneity test results are shown in Table 2.

Table 2 presents the estimation results of the benchmark regression and five robustness and endogeneity tests, comprehensively verifying that the spatial spillover effect of digital inclusive finance on regional indus trial development has high statistical robustness. The benchmark regression (three-dimensional coupling matrix) results show that the coefficient of the core explanatory variable is 0.318, the spatial autoregression coefficient is 0.218, and the spillover effect coefficient is as high as 0.384, all of which are significant at the 1% level, initially establishing the strong spillover characteristics of digital inclusive finance in the multi-dimensional spatial network of "geography-industry-finance". In the robustness test, after replacing the explained variable with total factor productivity, the coefficient of the core explanatory variable rose to 0.418, and the spillover effect coefficient is 0.371, indicating that the effect of digital finance on improving industrial efficiency is even stronger than its direct boost to the comprehensive industrial index. After binarizing the three-dimensional coupling matrix, the coefficients of the core independent variable and the spillover effect coefficient both slightly decreased to 0.302 and 0.351 respectively, indicating that the conclusion is not dependent upon the particular configuration of the weight strength for any of these four municipalities. After the removal of the municipalities, the core explanatory variable coefficient is now 0.365, while the spillover effect coefficient is now 0.376; although the coefficients are reduced significantly without sacrificing the overall structure of the estimates or the overall estimation structure. With respect to endogeneity testing, using two-stage least squares (2SLS) the core explanatory variable coefficients increase to 0.394 and the spillover coefficients reach 0.403. Using systematic GMM, the core explanatory variable coefficients are 0.386 and the spillover effect coefficient is 0.392 both again above the base regression; thus the general upward skewness in the coefficient distribution maintains the integrity of establishing causal identification. Throughout all test procedures, R2 remains stable above 0.75 and observes values for all model fits from 770-880 resulted in good agreement on consistency with the sample structure.

IV. CONCLUSION

This paper overcomes the limitations of traditional spatial analysis that relies on a single geographical weight by integrating a three-dimensional coupled weight matrix of geographical proximity, industrial chain linkage, and financial flow networks. Using a dynamic spatial Durbin model and spatiotemporal geographical weighted regression, it reveals that the spatial spillover effect of digital inclusive finance is significantly enhanced in the "geography-industry-finance" multidimensional network. At the end of the sample period, it initially exhibits a "spillover-dominated" characteristic, with core cities as hubs and spillover intensity decreasing in tiers with network location. This aligns with the heterogeneous pattern in the core-periphery structure where the spillover effect of core cities is significantly higher than that of peripheral cities. Social network analysis further identifies the alleviation of financing constraints as the core transmission mechanism among the three mediating paths. The study confirms that the multidimensional spatial framework can more accurately estimate the radiation boundary and transmission path of digital finance, providing policy insights for regional collaborative development from "geographical proximity" to "network linkage."

AUTHOR CONTRIBUTIONS

Conceptualization – Rui Ding and Qingjun Zeng; methodology – Rui Ding and Qingjun Zeng; investigation – Rui Ding and Qingjun Zeng; writing-original draft preparation – Rui Ding and Qingjun Zeng. All authors have read and agreed to the published version of the manuscript.

CONFLICTS OF INTEREST

The authors declare no conflict of interest.

FUNDING

This research was supported by,

Key Project of Chongqing Municipal Education Commission: Research on the Mechanism and Path of Intercity Industrial Synergistic Development in the Chengdu-Chongqing Economic Circle(21SKGD078); Chongqing

Social Science Planning Project "Research on the Mechanisms and Pathways for the Synergistic Enhancement of the New International Land-Sea Trade Corridor and Chongqing's Open Economy" (2024BS062); Chongqing Municipal Education Commission Humanities and Social Science Research Planning

Project "Research on the New International Land-Sea Trade Corridor Boosting Chongqing's Development into an Inland Open Comprehensive Hub" (25SKGH121)

ACKNOWLEDGEMENTS

Not applicable.

TABLE 2. Summary of robustness and endogeneity test results

Test Type	Core Coefficient	Standard Error	Spatial Autoregressive Coefficient	Spillover Effect Coefficient	R^2	Observations
Baseline regression (Three-dimensional coupling matrix)	0.318***	0.047	0.218***	0.384***	0.784	880
Robustness test 1: Alternative dependent variable (Total factor productivity)	0.418***	0.054	0.223***	0.371***	0.769	880
Robustness test 2: Alternative spatial weight matrix (Binarization of three-dimensional matrix)	0.302***	0.050	0.196***	0.351***	0.756	880
Robustness test 3: Excluding four municipalities directly under the central government	0.365***	0.052	0.208***	0.376***	0.781	848
Endogeneity test 1: Instrumental variable method (2SLS)	0.394***	0.063	0.231***	0.403***	0.772	880
Endogeneity test 2: System GMM estimation	0.386***	0.058	0.214***	0.392***	0.768	770

REFERENCES

[1] J. Li and B. Li, "Digital inclusive finance and urban innovation: Evidence from China," Review of Development Economics, vol. 26, no. 2, pp. 1010-1034, 2022, doi: 10.1111/rode.12846.
[2] B. Guo, Y. Feng, and J. Lin, "Digital inclusive finance and digital transformation of enterprises," Finance Research Letters, vol. 57, no. 1, pp. 104270-104278, 2023, doi: 10.1016/j.frl.2023.104270.
[3] Y. Bu, X. Du, Y. Wang, et al., "Digital inclusive finance: a lever for SME financing? " International Review of Financial Analysis, vol. 93, no. 1,pp. 103115-103127, 2024, doi: 10.1016/j.irfa.2024.103115.
[4] Q. Song, M. Yan, S. Tang, et al., "Digital financial inclusion and common prosperity in China: Spatial spillovers and regional divergence," Finance Research Letters, vol. 1, no. 1, pp. 109624-109634, 2026, doi: 10.1016/j.frl.2026.109624.
[5] M. Ai, W. Zhang, Z. Jiang, et al., "The impact of digital inclusive finance on urban economic resilience: Evidence from China," Finance Research Letters, vol. 68, no. 1, pp. 100084-100092, 2025, doi: 10.1016/j.dsef.2025.100084.
[6] Y. He, Y. Pan, and X. Yuan, "Whether Financial Inclusion Improves Employment Structure and Labor Allocation: Evidence From China's Industrial Restructuring," SAGE Open, vol. 15, no. 2, pp. 1-18, 2025, doi: 10.1177/21582440251340215 .
[7] Y. Huang, J. Zhao, and S. Yin, "Does digital inclusive finance promote the integration of rural industries? Based on the mediating role of financial availability and agricultural digitization," PloS one, vol. 18, no. 10, Art. no. e0291296, 2023, doi: 10.1371/ journal.pone.0291296.
[8] Y. Chen and L. Zhan, "Digital inclusive finance and intercity innovation collaboration: moderating effects of digital infra structure and polycentricity," Applied Economics Letters, vol. 1, no. 1, pp. 1-8, 2025, doi: 10.1080/13504851.2025.2563786.
[9] Z. Sun, C. Cao, Z. He, et al., "Examining the coupling coordination relationship between digital inclusive finance and technological innovation from a spatial spillover perspective: Evidence from China," Emerging Markets Finance and Trade, vol. 59, no. 4, pp. 1219-1231, 2023, doi: 10.1080/1540496x.2022.2120766.
[10] L. Chen and G. Zhang, "Exploring the Impact of Digital Inclusive Finance and Industrial Structure Upgrading on High-Quality Economic Development: Evidence from a Spatial Durbin Model," Economies, vol. 13, no. 8, pp. 212-221, 2025, doi: 10.3390/economies13080212.
[11] F. Janatabadi and A. Ermagun, "Access weight matrix: a place and mobility infused spatial weight matrix," Geographical Analysis, vol. 56, no. 4, pp. 746-767, 2024, doi: 10.1111/gean.12395.
[12] P. Hui, H. Zhao, D. Liu, et al., "How does digital finance affect regional innovation capacity? A spatial econometric analysis," Economic Modelling, vol. 122, no. 1, pp. 106250-106261, 2023, doi: 10.1016/j.econmod.2023.106250.
[13] H. Dong, M. Du, and X. Zhou, "Spatial-Temporal Differentiation and Dynamic Evolution of Digital Finance Inclusive Development in the Yangtze River Delta Economic Cluster of China," Mobile Information Systems, vol. 2022, no. 1, pp. 5470373-5470381, 2022, doi: 10.1155/2022/5470373.
[14] R. Ding, F. Shi, and S. Hao, "Digital inclusive finance, environmental regulation, and regional economic growth: An empirical study based on spatial spillover effect and panel threshold effect," Sustainability, vol. 14, no. 7, pp. 4340-4348, 2022, doi: 10.3390/su14074340.
[15] L. Chen and G. Zhang, "Research on the impact of digital financial inclusion and environmental regulation on industrial structure upgrading-based on spatial Durbin model analysis," Plos one, vol. 19, no. 11, Art. no. e0310720, 2024, doi: 10.1371/ journal.pone.0310720.
[16] C. Yu, N. Jia, W. Li, et al., "Digital inclusive finance and rural consumption structure–evidence from Peking University digital inclusive financial index and China household finance survey," China Agricultural Economic Review, vol. 14, no. 1, pp. 165-183, 2022, doi: 10.1108/caer-10-2020-0255.
[17] W. Yu, H. Huang, X. Kong, et al., "Can Digital Inclusive Finance Improve the Financial Performance of SMEs? " Sustain ability, vol. 15, no.3, pp. 1867-1876, 2023, doi: 10.3390/su15031867 .
[18] S. Laqueur H, B. Shev A, and C. Kagawa R M, "SuperMICE: an ensemble machine learning approach to multiple imputation by chained equations," American journal of epidemiology, vol. 191, no. 3, pp. 516-525, 2022, doi: 10.1093/aje/kwab271.
[19] M. Hasanah and A. Suharso, "Algoritma Haversine pada Sistem Informasi Geografis: Tinjauan Literatur Sistematis: Tinjauan Literatur Sistematis," Nuansa Informatika, vol. 17, no. 2, pp. 135-143, 2023, doi: 10.25134/ilkom.v17i2.10.
[20] A. Muttaqin, A. Murtopo, S. Syefudin, et al., "Application of the haversine formula method to determine the closest distance to a minimarket," Jurnal Mandiri IT, vol. 13, no. 1, pp. 72-80, 2024, doi: 10.35335/mandiri.v13i1.293.
[21] V. Holy and K. Safr, "Disaggregating input–output tables by the multidimensional RAS method: A case study of the Czech Republic," Economic Systems Research, vol. 35, no. 1, pp. 95-117, 2023, doi: 10.1080/09535314.2022.2091978.
[22] O. Henriques C and S. Sousa, "A review on economic input-output analysis in the environmental assessment of electricity generation," Energies, vol. 16, no. 6, pp. 2930-2941, 2023, doi: 10.3390/en16062930.
[23] K. Oanh T T, "Digital financial inclusion in the context of financial development: Environmental destruction or the driving force for technological advancement," Borsa Istanbul Review, vol. 24, no. 2, pp. 292-303, 2024, doi: 10.1016/ j.bir.2024.01.003.
[24] A. Johri, M. Asif, P. Tarkar, et al., "Digital financial inclusion in micro enterprises: understanding the determinants and impact on ease of doing business from World Bank survey," Humanities and Social Sciences Communications, vol. 11, no. 1, pp. 1-10, 2024, doi: 10.1057/s41599-024-02856-2.
[25] J. John, M. Bellingeri, D. Lekha, et al., "Effect of Weight Thresholding on the Robustness of Real-World Complex Networks to Central Node Attacks," Mathematics, vol. 11, no. 16, pp. 3482-3489, 2023, doi: 10.3390/math11163482.
[26] X. Wang and Z. Wang, "Identifying influential nodes in weighted complex networks by considering the importance of shortest paths," Journal of Big Data, vol. 12, no. 1, pp. 100-126, 2025, doi: 10.1186/s40537-025-01159-w.
[27] T. Inoha, K. Sadakane, Y. Uno, et al., "Efficient computation of betweenness centrality by graph decompositions and their applications to real-world networks," IEICE TRANSACTIONS on Information and Systems, vol. 105, no. 3, pp. 451-458, 2022, doi: 10.1587/transinf.2021fcp0003.
[28] B. Kaminski, P. Misiorek, P. Pralat, et al., "Modularity based community detection in hypergraphs," Journal of Complex Networks, vol. 12, no. 5, pp. cnae041, 2024, doi: 10.1093/comnet/cnae041.
[29] S. Hairol Anuar, Z. Abas, N. Yunos, et al., "Identifying Communities with Modularity Metric Using Louvain and Leiden Algorithms," Pertanika Journal of Science & Technology, vol. 32, no. 3, pp. 1285-1300, 2024, doi: 10.47836/pjst.32.3.16 .

[30] H. Zhong, J. Zhang, and W. Song, "The relationship between rural information consumption and regional economic development with spatial Durbin model—A case study of Zhejiang, China," Plos one, vol. 18, no. 2, Art. no. e0281405, 2023, doi: 10.1371/journal.pone.0281405.

[31] M. Koley and AK. Bera "To use, or not to use the spatial Durbin model?– that is the question," Spatial Economic Analysis, vol. 19, no. 1, pp. 30-56, 2024, doi: 10.1080/17421772.2023.2256810.

[32] H. Yu, "Generalized geographically and temporally weighted regression," Computers, Environment and Urban Systems, vol. 117, no. 1, pp. 102244-102256, 2025, doi: 10.1016/j.compenvurbsys.2024.102244.

[33] W. Tu, C. Rao, X. Xiao, et al., "Interactive geographical and temporal weighted regression to explore spatiotemporal characteristics and drivers of carbon emissions," Environmental Technology & Innovation, vol. 36, no. 1, pp. 103836-103842, 2024, doi: 10.1016/j.eti.2024.103836.

[34] Y. Chen, "Spatial autocorrelation equation based on Moran's index," Scientific reports, vol. 13, no. 1, pp. 19296-19299, 2023, doi: 10.1038/s41598-023-45947-x.

[35] H. Yamada, "Moran's I for multivariate spatial data," Mathematics, vol. 12, no. 17, pp. 2746-2757, 2024, doi: 10.3390/ math12172746 .